Simultaneous Two-Way Doppler and Ranging for Multiple Spacecraft at Mars: Flight Radio Tracking System Design and Performance Simulations[1]

Kar-Ming Cheung[2], Dariush Divsalar[3]
Jet Propulsion Laboratory, California Institute of Technology, 4800 Oak Grove Drive, Pasadena CA 91109, USA

Mars exploration requires multiple orbiters and surface infrastructures on Mars. Location determination is essential to support various human and robotic activities on the Mars surface and in orbits. Robust communication coverage is required for data transmission between assets on Mars surface and orbiters in addition to the communication between orbiters and Earth. We proposed a notional Mars Regional Navigation Satellite System (MRNSS) that provides continuous or near-continuous in-situ navigation and timing services for the robotic and human missions in the vicinity of a Mars landing site. For such a system, the Earth's deep space stations have to perform orbit determination (OD) for the Mars orbiters so that their locations are known to a reasonable degree of accuracy. This provides the surface and orbiting user vehicles the ability to estimate their locations using the orbiter-vehicle range measurements. Two important inputs for accurate OD are 2-way Doppler and ranging measurements derived from the transmitted and received radio signals. We also introduced a new flight-ground collaborative architecture that provides simultaneous Doppler and ranging measurements for multiple spacecraft in the Mars vicinity, using an example of the Mars landing site Utopia Planitia and four Mars orbiters, all communicating with Earth via two-way communications in the X-band frequency range. One key component of this architecture is that each spacecraft uses a smart frequency sweeping algorithm that acquires and tracks the uplink signals with high Doppler and Doppler rate residuals. In this paper, we simulate the Doppler and Doppler rate profiles of the Mars orbiters of the MRNSS and assessed the acquisition and tracking performances.

I. Introduction

HUMAN Mars explorations require substantial build-up of orbiting and surface infrastructures on Mars. In addition to communication coverage, location awareness is essential to support various human and robotic activities on the Mars surface and on orbits. In [1], we proposed to leverage on the planned Mars orbiting assets, and to establish a Mars Regional Navigation Satellite System (MRNSS) that provides continuous or near-continuous in-situ navigation and timing services for the robotic and human missions in the vicinity of the Mars landing site.

One challenge to the MRNSS concept is that in order for the user vehicles to estimate their locations using the orbiter-vehicle range measurements, the Earth's deep space antennas have to perform orbit determination (OD) for the Mars orbiters so that their locations are known to a reasonable degree of accuracy. The traditional approach of tying up one ground antenna to one Mars orbiter to perform 2-way Doppler and ranging measurements can be problematic, when there are 4 or more Mars orbiters that requires OD tracking support at the same time.

In [2], we leveraged on prior work [3] that focus on simultaneous command and telemetry links and introduced a new flight-ground collaborative architecture that provides simultaneous Doppler and ranging for multiple spacecraft in the Mars vicinity. We assumed that 2-way ranging is done in X-band, which also supports low-rate command and telemetry. The operational Deep Space Network (DSN)'s Multiple-Spacecraft-Per-Antenna (MSPA) method is basically a static Frequency Division Multiple Access (FDMA) scheme. For *N* Mars orbiters, the downlinks operate in N allocated frequency bands separated by *N-1* guard bands to prevent interferences. On the other hand, the uplinks

[2] Group Supervisor, Telecommunications Architectures
[3] Engineering Fellow, Information Processing

received by the *N* orbiters exhibit different Doppler and Doppler rate effects due to their different dynamics with respect to Earth.

To enable simultaneous Doppler and ranging measurements, we propose the following updates to the existing flight and ground systems and the frequency allocation process:

1) The *N* spacecraft time-share a single uplink frequency—we assumed that each spacecraft is capable to acquire and to track the same Doppler-compensated uplink (to be discussed later), which is shared among all spacecraft. This approach on uplink was also recommended for the Multiple-Uplink-Per-Antenna (MUPA) concept [4].
2) The ground "Doppler-compensates" the uplink signal in either one of the following ways: i) with respective to the Mars center, or ii) with respect to the average of Doppler profiles of the *N* orbiters. The guard bands have to be wide enough to accommodate the residual Dopplers between the frequency-adjacent orbiters. Using the MRNSS scenario in [1], simulation results show that the residual Doppler and residual Doppler rate are bounded by 40 KHz and 2.6 Hz/s respectively.
3) On the spacecraft side, the Command and Data Handling (C&DH) subsystem of each spacecraft has to be able to identify its own uplink commands and data loads on the uplink data stream using its unique spacecraft Identifier (SCID). The onboard radio would require the following upgrades:
    a. A different turn-around ratio for each spacecraft so that the same Doppler-compensated uplink signal received by each spacecraft would be coherently "turned around" to modulate the telemetry and ranging signals on a different downlink frequency.
    b. A well-designed tracking loop that can sweep, acquire, and track the unknown uplink carrier phase and residual Doppler and Doppler rate. A preliminary design of this type of tracking loop was introduced in [5] for use by a constellation of 20 spacecraft in a halo orbit around the Earth-Moon Lagrange Point L1. In [2], we introduced a smart sweeping algorithm that uses multiple thresholds and frequency step sizes for sweeping and compares current and previous measurement values to determine the sweeping direction.
4) On the frequency allocation side, the guard bands have to be wide enough to ensure that adjacent ranging signals do not interfere with one another.

In this paper, we simulate the Doppler and Doppler rate of the Mars orbiters during the human-Mars era and assessed the acquisition and tracking performances of the onboard system. The ground antenna system is basically unchanged and tracks multiple downlink signal streams from different Mars assets using MSPA. Multiple Receiver Ranging Processors (RRP's) at the ground station are used to measure the Doppler frequency and estimate the range. The details of the ground system are discussed in [6] and will not be discussed in this paper.

The rest of the paper is organized as follows: Section II describes the notional MRNSS architecture. Section III discusses the Doppler and Doppler rate simulations and provides the statistics. Section IV introduces the flight tracking system, and describes the smart frequency sweeping algorithm. Section V discusses the acquisition and tracking performances of the MRNSS scenario. Section VI provides concluding remarks.

II. A Notional Mars Regional Navigation Satellite System (MRNSS)

The MRNSS architecture was described in [1], but for the sake of gathering all the relevant information of this paper in one place, we discuss the architecture again in this section.

We consider the scenario of a Human Mars landing site at Utopia Planitia on Mars, and propose a navigation satellite constellation that provides navigation and timing services in the surrounding region of the landing site. The navigation satellite constellation leverages on the two planned areostationary relay orbiters (Aero45 and Aero90) and the Deep Space Habitat (DSH) in a circular 48-hour inclined orbit (Mars48hr), and augmented it with a notional navigation satellite in an areosynchronous orbit that traces around a figure-8 path (Aero68). The notional Mars landing site location and orbiters' orbital parameters are given as follows:

- Utopia Planitia: 182.5° due East, 46.7° due North
- Aerostationary orbiter 1 (Areo45): 162.5° due East
- Aerostationary orbiter 2 (Areo90): 207.5° due East
- Aerosynchronous orbiter (Areo68): 180° due East and 20° inclined
- Deep Space Habitat (Mars48hr): 180° due East, 149.5° inclined

The orbits of the proposed Mars navigation nodes are shown in Figure 1 (3-D view), and the projections of these orbits onto the Mars surface are shown in Figure 2 (2-D view). Note that in Figure 2 the Mars navigation nodes cluster together, and Utopia Planitia is north of the cluster. The satellite-receiver geometry appears to be weak and the

geometric dilution of precision (GDOP) is high. In other words, the localization solution can be very sensitive to the errors in the raw-range measurements. The detailed system concept is described in [1].

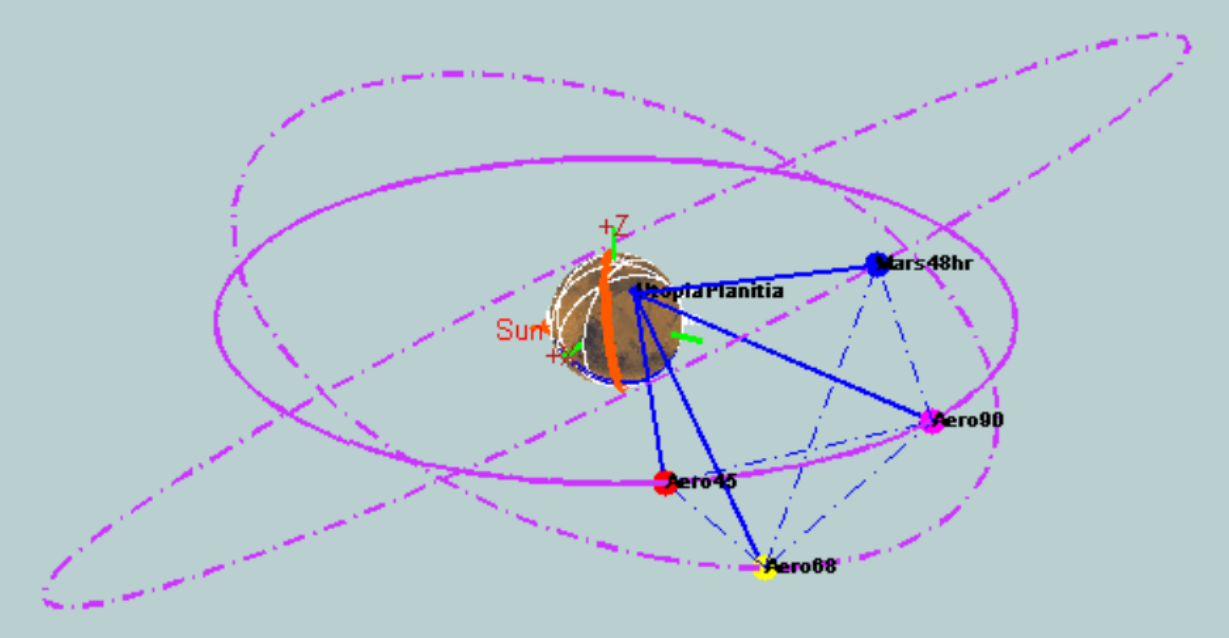

Fig. 1 Orbits of the Notional Mars Navigation Nodes (3-D View).

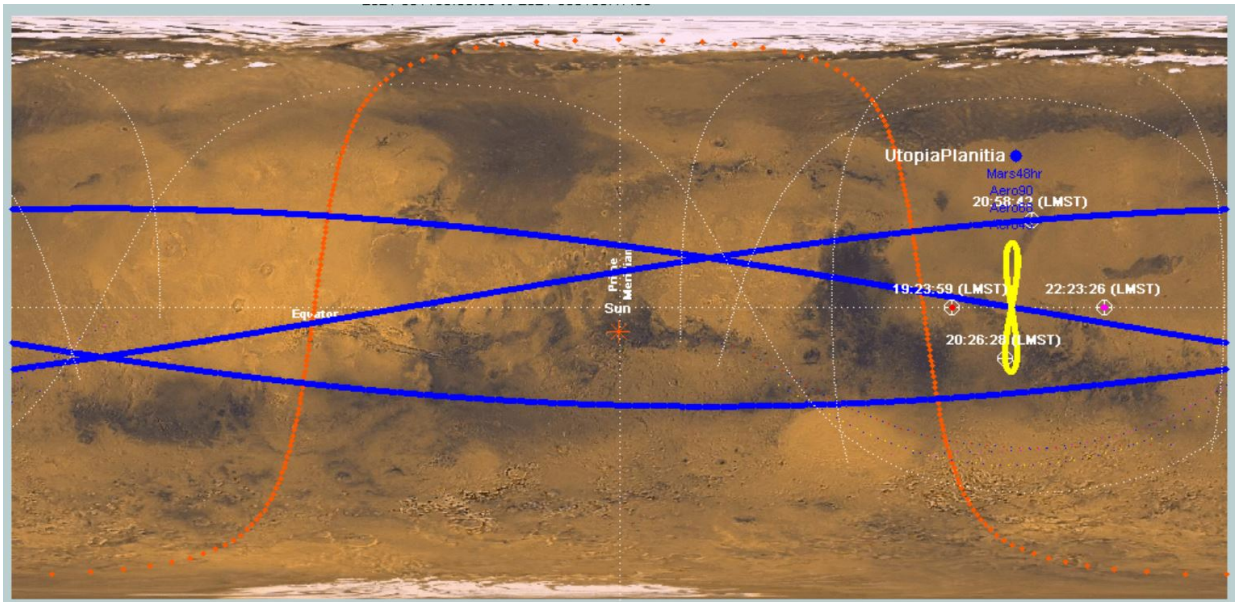

Fig. 2 Orbits of the Notional Mars Navigation Nodes (2-D View).

III. Doppler and Doppler Rate Simulations and Statistics for the MRNSS

As discussed in earlier sections, we assume 2-way Doppler and ranging are done in X-band. The relative motion between an Earth antenna and a Mars orbiter causes the received frequency to differ from the transmitted frequency. In the traditional case of one Earth antenna tracking a single spacecraft (one-on-one), the DSN constantly tunes the

uplink carrier signal to compensate for the Doppler effect, thus providing a near-constant received frequency that is close to the best lock frequency to assist carrier signal acquisition by the spacecraft. For the proposed scheme of transmitting one uplink signal to multiple spacecraft, each spacecraft experiences different Doppler and Doppler rate effects due to their different dynamics relative to the Earth's ground station. We propose the following collaborative flight-ground architecture for simultaneous 2-way Doppler and ranging: the ground antenna "Doppler compensates" the uplink carrier signal with either one of the following ways: i) with respect to the Mars center, or ii) with respect to the average of Doppler profiles of all the spacecraft. This ensures that the residual Doppler frequencies and Doppler rates as experienced by all the spacecraft are comparable. On the flight side, the radio on each spacecraft sweeps, acquires, and tracks the unknown uplink carrier phase and residual Doppler frequency. Using the above proposed MRNSS scenario, we simulate the Doppler's and Doppler rates of the four orbiters and the landing site Utopia Planitia for 8 days and compare with the Doppler frequencies and Doppler rates of the Mars center and the Doppler centroid. A 30-hour time profile of the simulations is shown in Figure 3. The maximum residual Doppler and Doppler rate as experienced by each spacecraft using the Doppler compensation strategies of i) Mars center and ii) Doppler centroid are shown in Figures 4 and 5 respectively.

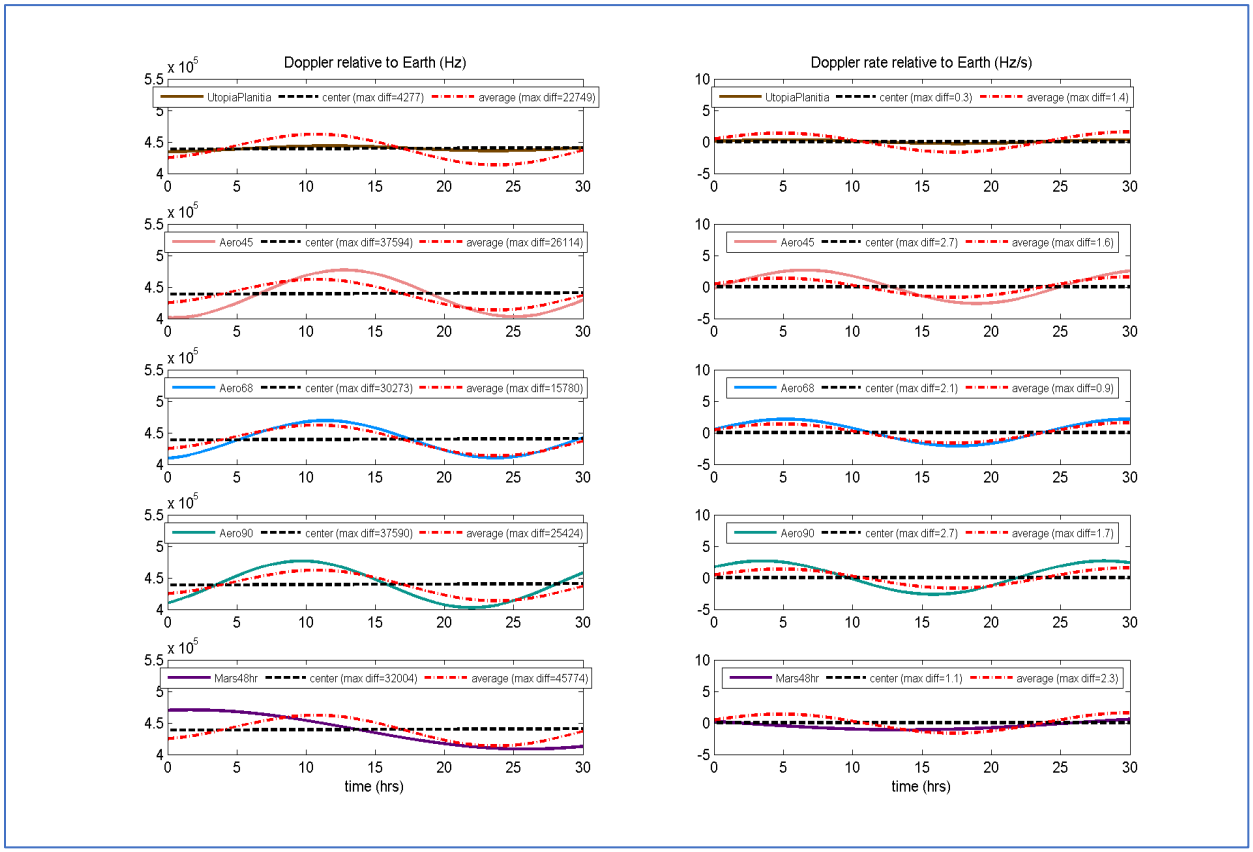

Fig. 3 30-Hour Time Profiles of Doppler and Doppler Rate (8-Day Simulation).

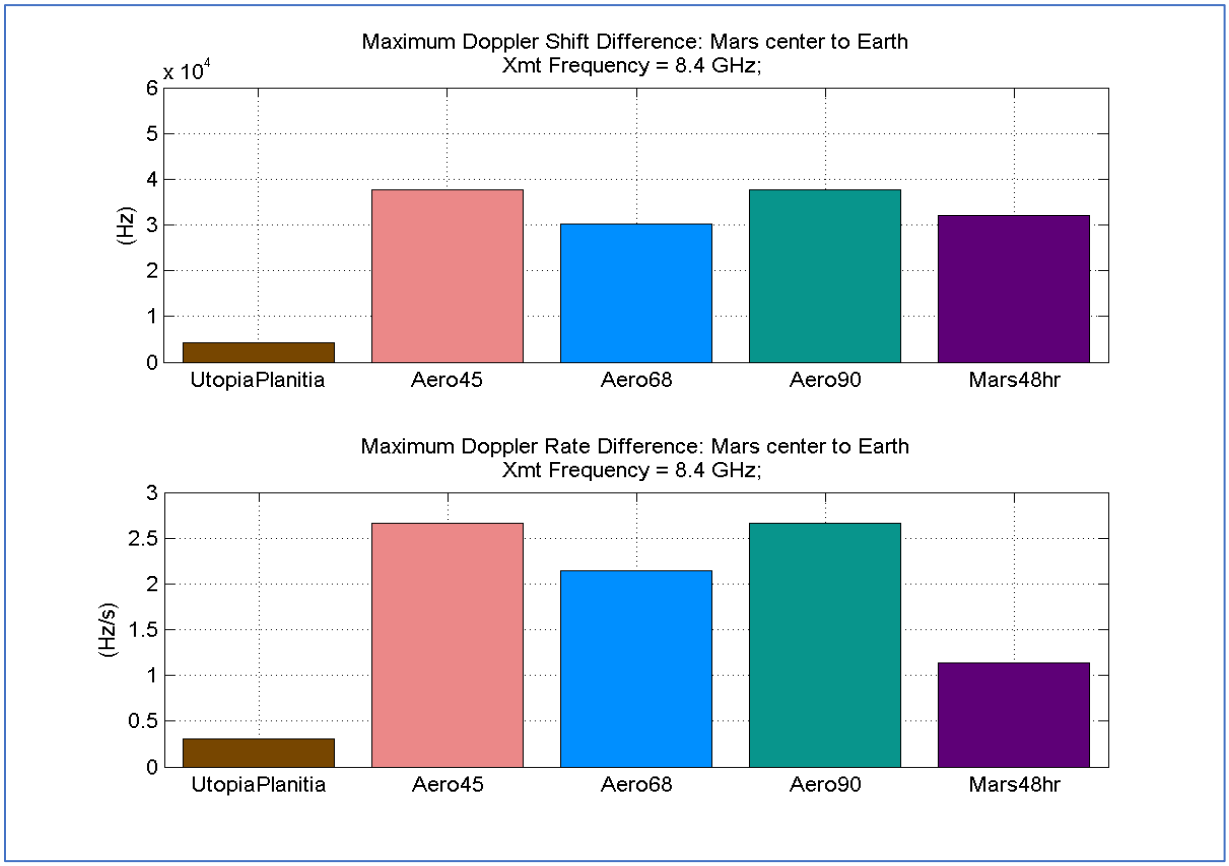

Fig. 4 Maximum Residual Doppler/Doppler rate Using Mars Center Compensation Strategy

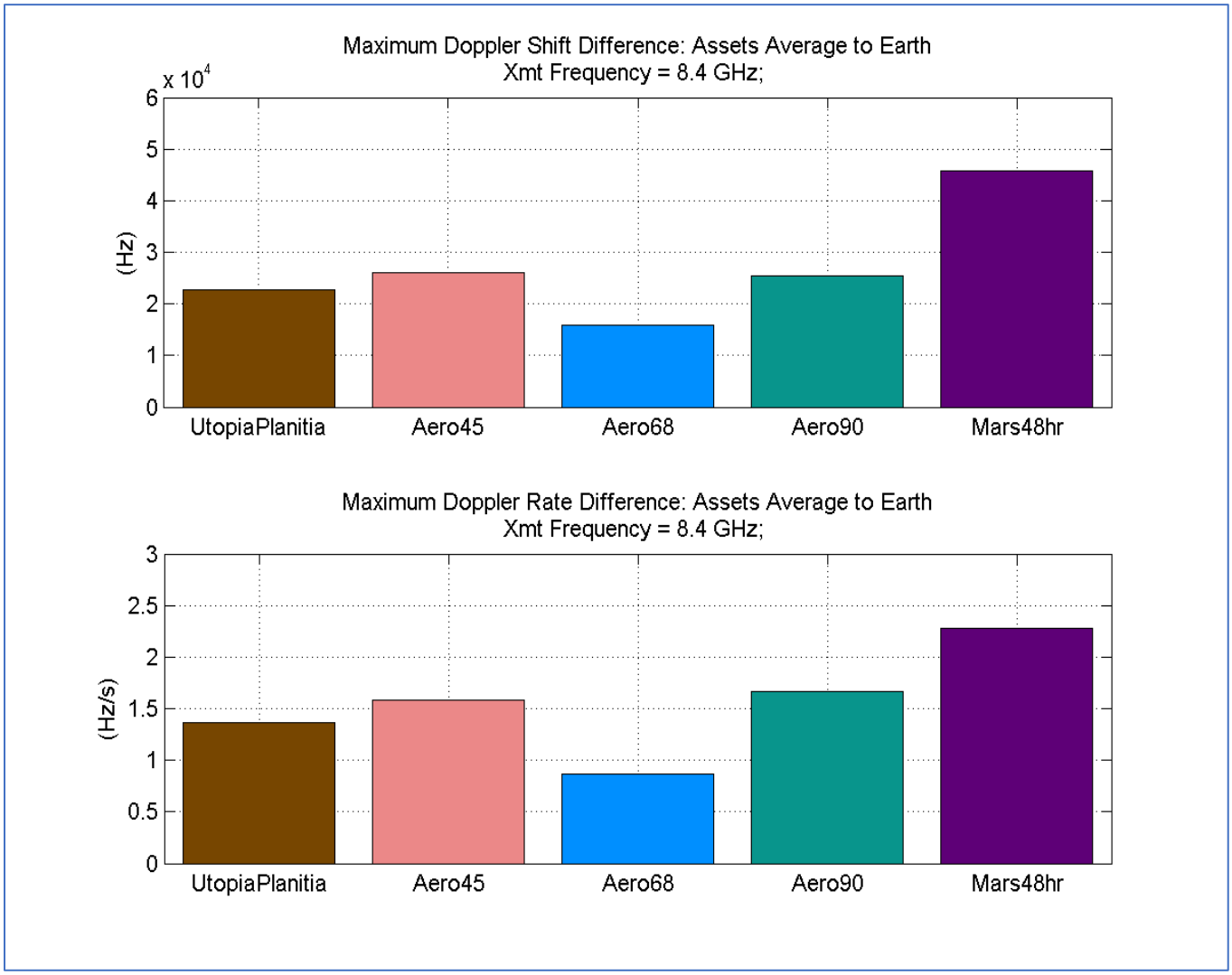

Fig. 5 Maximum Residual Doppler/Doppler rate Using Doppler Centroid Compensation Strategy.

IV. Flight Tracking System

In this section the structure of uplink and downlink signals will be reviewed and are briefly discussed. The transmitted uplink signal can be written as

$$S_T(t) = \sqrt{2}\,\sin[2\pi\alpha_U f_T t + \theta\, p_c(t)\sin(2\pi\frac{R_c}{2}t)] \quad (1)$$

where f_T is the uplink carrier frequency, α_U is a function of time that accounts for the Doppler effect on the uplink, $p_c(t)$ is the ranging signal taking values of ± 1 with chip rate R_c and θ is ranging modulation index. The range clock is $\frac{R_c}{2} = \alpha_U \beta f_T$ where

$$\beta = 2^{-7-C} \qquad \text{for S-band uplink}$$
$$\beta = \frac{221}{749}2^{-7-C} \qquad \text{for X-band uplink} \tag{2}$$

and C is an integer to be defined in the next section. Thus, the range clock also experiences a Doppler effect and appears at the spacecraft with a frequency $\alpha_U \beta f_T$. Therefore, the ranging signal is coherently related to the carrier frequency, which is a requirement for Doppler rate aiding. The uplink signal can be further represented as

$$S_T(t) = \sqrt{2}\,\sin[2\pi\alpha_U f_T t]\cos[\theta\, p_c(t)\sin(2\pi\frac{R_c}{2}t)]$$
$$+\cos[2\pi\alpha_U f_T t]\sin[\theta\, p_c(t)\sin(2\pi\frac{R_c}{2}t)]$$

But

$$\cos[\theta\, p_c(t)\sin(2\pi\frac{R_c}{2}t)] = J_0(\theta)$$
$$+2\sum_{k=1}^{\infty} J_{2k}(\theta)\cos(4k\pi\frac{R_c}{2}t)$$

and

$$\sin[\theta\, p_c(t)\sin(2\pi\frac{R_c}{2}t)] =$$
$$2p_c(t)\sum_{k=1}^{\infty} J_{2k-1}(\theta)\cos(2(2k-1)k\pi\frac{R_c}{2}t)$$

where $J_k(\theta)$ is the k-th Bessel function of the first kind. Since higher ranging harmonics can be filtered

$$\cos[\theta\, p_c(t)\sin(2\pi\frac{R_c}{2}t)] \approx J_0(\theta)$$

and

$$\sin[\theta\, p_c(t)\sin(2\pi\frac{R_c}{2}t)] \approx 2p_c(t)J_1(\theta)\cos(2\pi\frac{R_c}{2}t)$$

Thus, the uplink signal after filtering can be represented as

$$S_T(t) = \sqrt{2}\,J_0(\theta)\sin[2\pi\alpha_U f_T t]$$
$$+\sqrt{2}\cos[2\pi\alpha_U f_T t]2J_1(\theta)p_c(t)\sin(2\pi\frac{R_c}{2}t) \tag{3}$$

The first term is residual carrier and can be tracked by a spacecraft radio with a phase locked loop (PLL) using a smart frequency sweeping algorithm (to be discussed shortly). We used complex signal representation for simplicity. The system block diagram at Spacecraft Radio is shown in Figure 6. In this Figure the bandwidth of Low Pass Filter (LPF) is slightly larger than maximum expected frequency difference $|\mathbf{f_{RX}} - \mathbf{f_{PLL}}|$ (denoted as $|\mathbf{f_{RX}} - \mathbf{f_{PLL}}|_{\mathbf{max}}$) where $\mathbf{f_{RX}}$ is the received Doppler and $\mathbf{f_{PLL}}$ is the estimated Doppler by PLL. This LPF also reduces the interference due to PN signal. The block diagram of phase locked loop (PLL) is shown in Figure 7.

Complex signal representation of SC RX

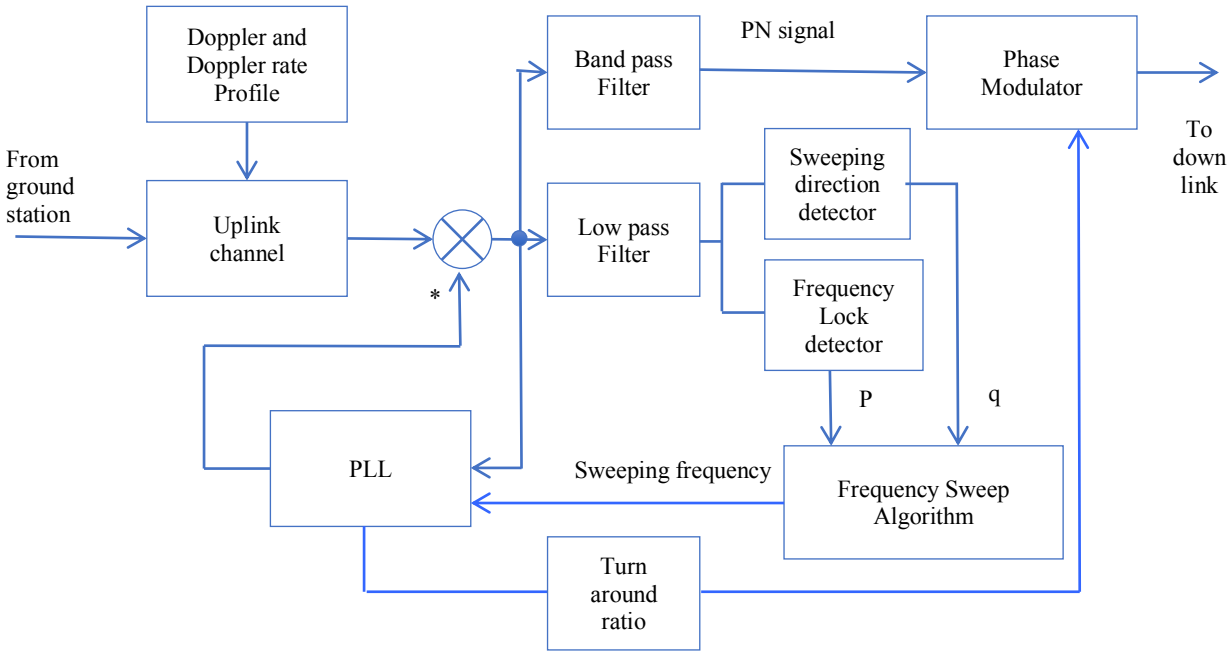

Fig. 6 Schematic of Spacecraft Radio

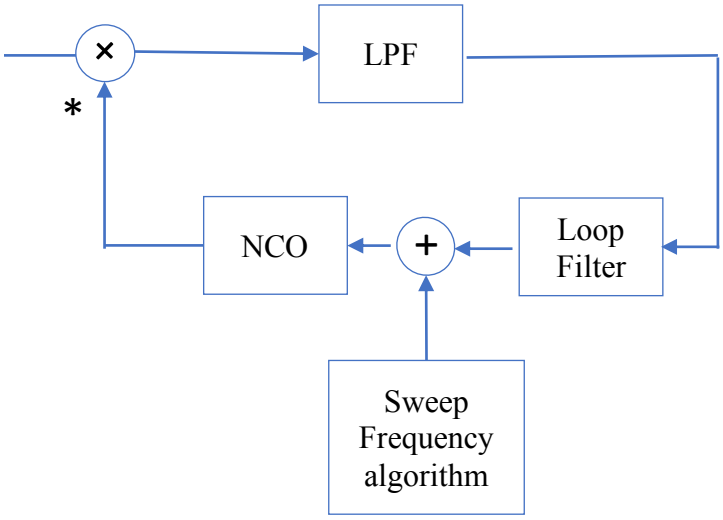

Fig. 7 Block Diagram of PLL

V. A New Smart Frequency Sweeping Scheme

The new frequency sweeping algorithm is a modified version of a smart frequency sweeping method described in [2]. The new smart frequency sweeping algorithm is shown in Figure 10. The signal P (taking values between 0 and 1 in absence of noise) is the output of frequency lock detector in Figure 6. The signal P is obtained by either integrating

M samples after the mixer during each frequency interval or equivalently using a low pass filter (LPF) as shown in Figure 8. The parameter M, or equivalently, the bandwidth of LPF should be chosen to maintain the lock stability.

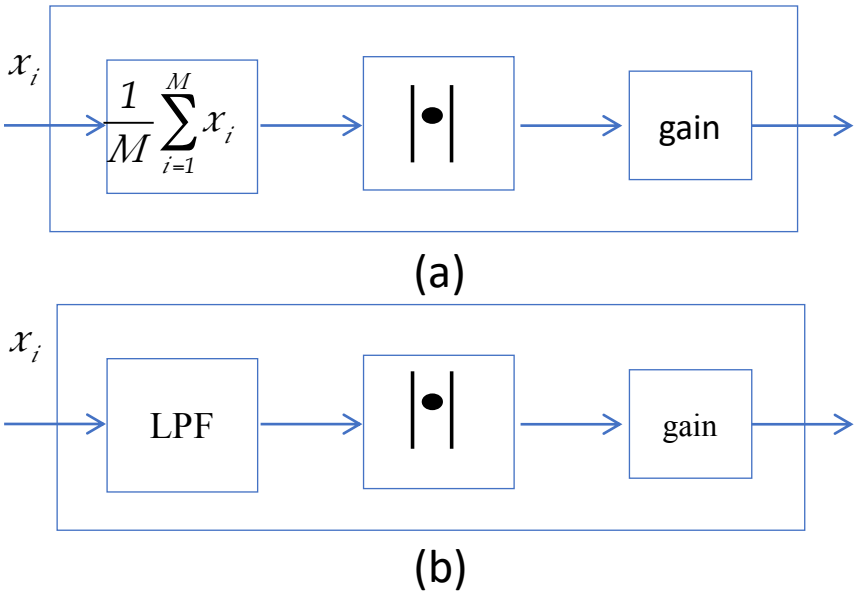

Fig. 8 Frequency Lock detector

In addition to signal P, a signal q (taking values +1 or −1), which is the output of sweeping direction detector in Figure 6, is introduced to provide the direction of the frequency sweep. The frequency direction detector is shown in Figure 9. Instead of and integrator, a LPF can be used in Figure 9. The parameter M' or the bandwidth of LPF should be chosen to provide an accurate estimate of frequency direction in the presence of noise. The delay should be smaller than the inverse of $4|\mathbf{f_{RX}} - \mathbf{f_{PLL}}|_{\mathbf{max}}$.

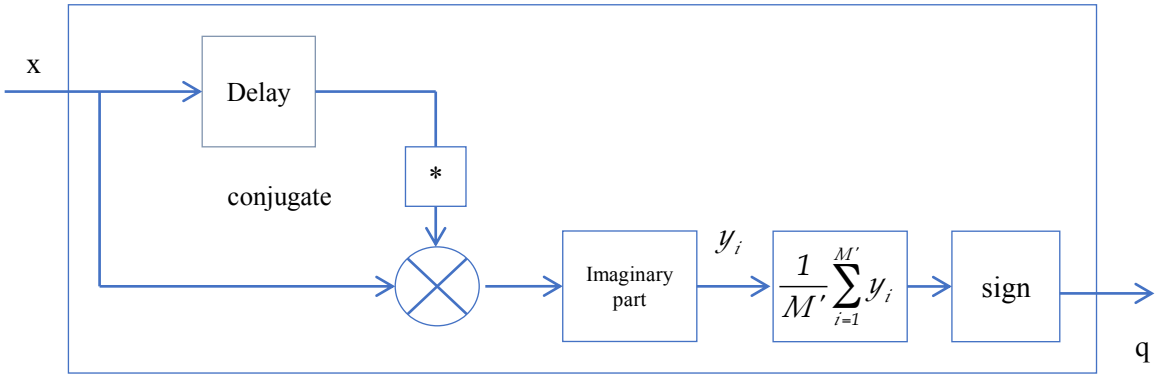

Fig. 9 Frequency direction detector

In contrast to the straightforward static and memoryless sweeping approach [7][8] that uses constant frequency step size and marches from a minimum frequency to a maximum frequency and repeats, we consider a more sophisticated but realizable algorithm that has the following characteristics:

1) It uses multiple thresholds and changes the frequency step size when the signal P is greater than a threshold.
2) It detects whether the received Doppler frequency is greater than the estimated Doppler frequency by PLL (q=+1) or is lower (q=−1) to determine the sweeping direction—either increase or decrease the sweeping frequency.

In Figure 10, the data flow on the left illustrates the dynamic sweeping circuit with multiple thresholds and frequency step sizes. The data flow on the right is the sweeping direction estimation signal that compares the difference between the received Doppler frequency and the estimated Doppler frequency by PLL. The plot on the left shows the

case of a PLL with the smart frequency algorithm acquires and tracks the Doppler frequencies in the range of −45 KHz to +45 KHz and Doppler rate of 2.6 Hz/sec. The signal can be acquired within seconds, and the frequency tracking error after acquisition is small compared to the loop bandwidth.

The frequency acquisition algorithm that controls the frequency sweep requires the range of frequency sweep to be defined through a start frequency f_1, a final frequency f_2, and a frequency step size f_{step} to increment or decrement the frequency.

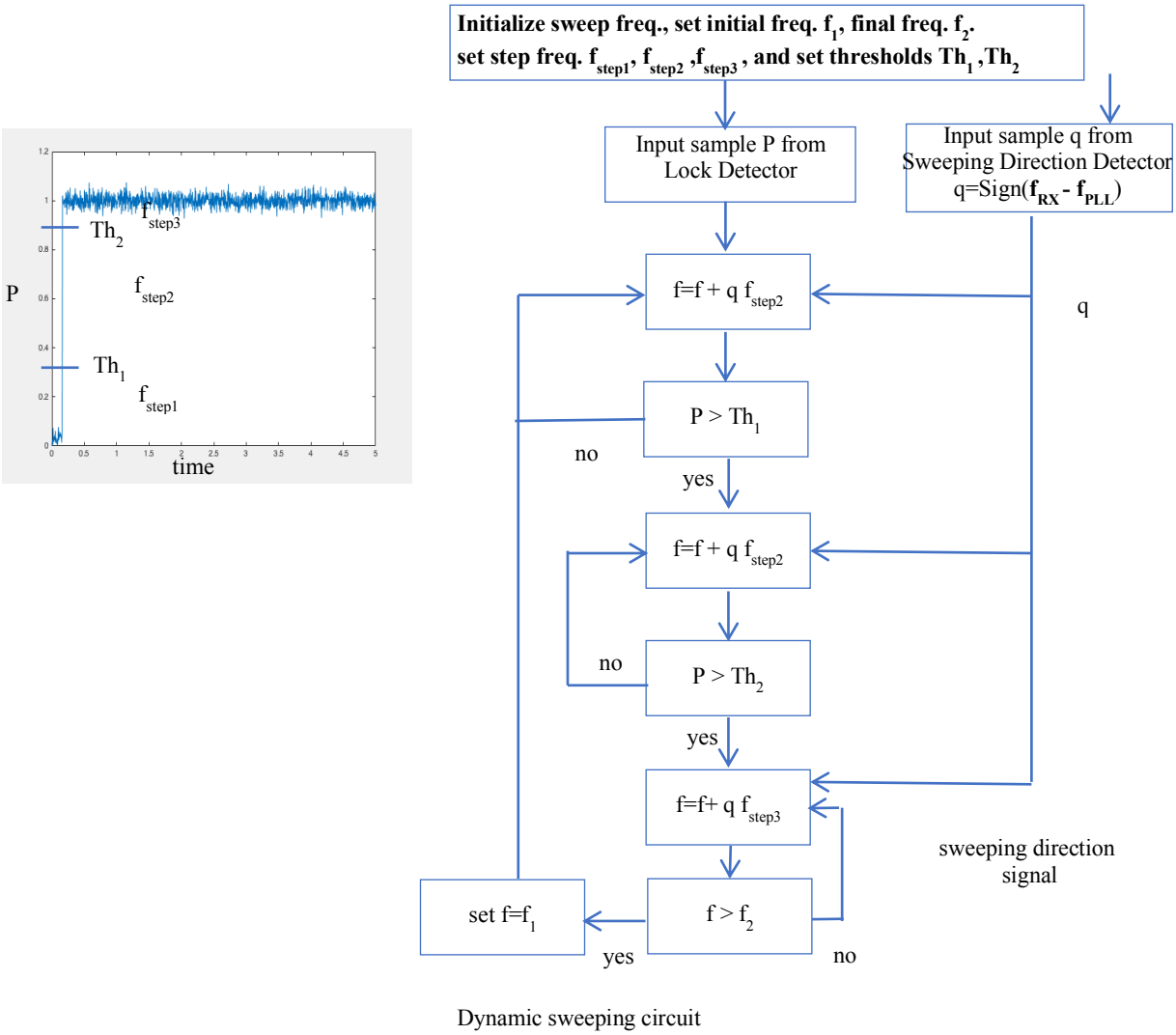

Fig. 10 A new Smart Frequency Sweeping Algorithm

VI. Acquisition and Tracking Performances of the MRNSS Scenario

We assume DSN 34-m BWG antenna with 20 kW uplink power, and 1-m parabolic dish antenna for the Mars orbiter at maximum Mars range. We divide equal power to the carrier and ranging channels. The conservative received carrier signal-to-noise ratio *Pc/No* is 52 dB. System Simulink model for spacecraft Radio is shown in Figure 11. Signals have complex representation. The frequency sweeping circuits, lock detector, and frequency direction circuits are also shown in Figure 11. Figure 12 shows the transmitted carrier with PN ranging block. The circuit for Phase locked loop (PLL) is shown in Figure 13. The Loop filter circuit with loop parameters is shown in Figure 14. The PLL also produces carrier with turned around ratio 221/749 that modulates the PN ranging to be transmitted to the downlink channel (not shown in the Simulink model). The threshold TH1 for Switch1 is set to 0.5. The threshold TH2 for Switch is set to 0.95. The initial frequency in Delay circuit is set to −50 KHz. Switch1 first

selects a frequency step of 50 Hz. When the signal P in Switch1 exceeds threshold TH1 of 0.5 the frequency step size is reduced to 1 Hz. The spectrum at the output of low pass filter for carrier tracking is shown in Figure 15. The spectrum at the output of band-pass filter for PN filtering and downlink modulation is shown in Figure 16 (PN filtering and down link modulation are not shown in the Simulink model). The PLL with the new smart frequency sweeping acquires and tracks the Doppler frequencies in range of −45 KHz to +45 KHz. In the simulations initial Doppler is assumed to be −20000 Hz and Doppler rate of 2.6 Hz/sec. We assumed loop bandwidth of 20 Hz. Lock detection signal P during frequency acquisition and tracking is shown in Figure 17. The difference between Doppler and PLL estimated Doppler during frequency acquisition and tracking is shown in Figure 18. The sign of this difference in signal represents the signal q. Frequency tracking error after acquisition and tracking is shown in Figure 19. The measured standard deviation of frequency error after acquisition is 6.2 Hz using loop bandwidth of 20 Hz. The Doppler and the PLL estimated Doppler are shown in Figure 20. As it can be seen in the Figure the PLL nicely tracks the initial Doppler with Doppler rate of 2.6 Hz/sec.

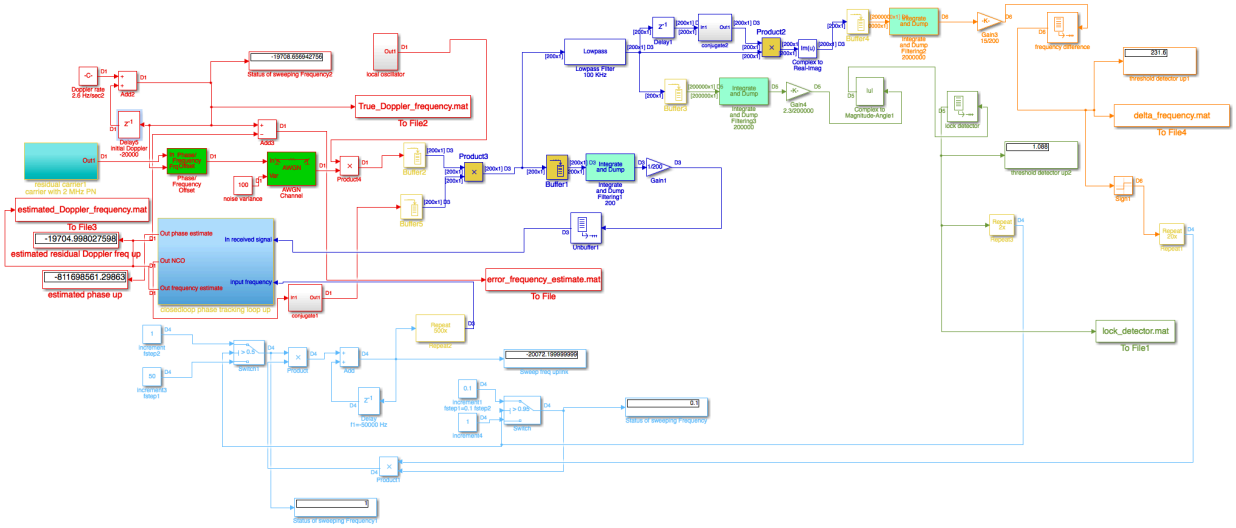

Fig. 11 Simulink model for spacecraft Radio

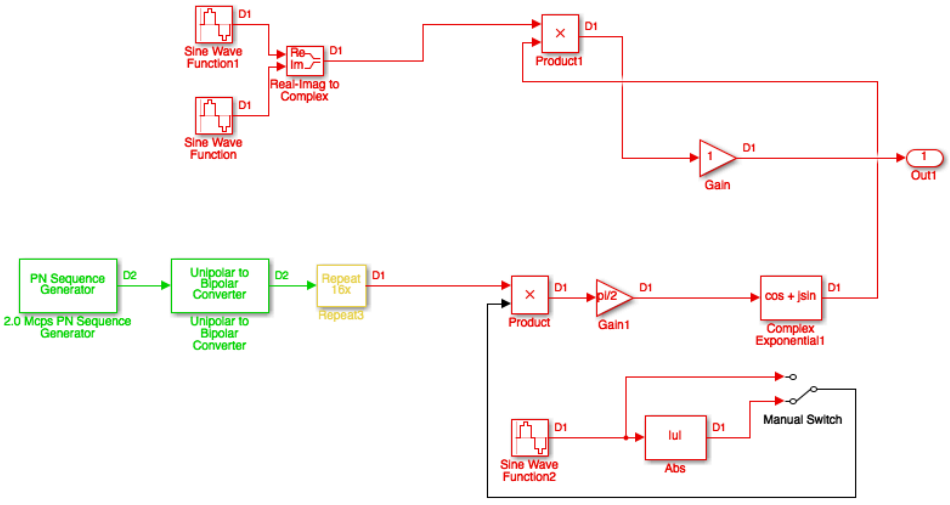

Fig. 12 Uplink transmitted carrier with PN ranging

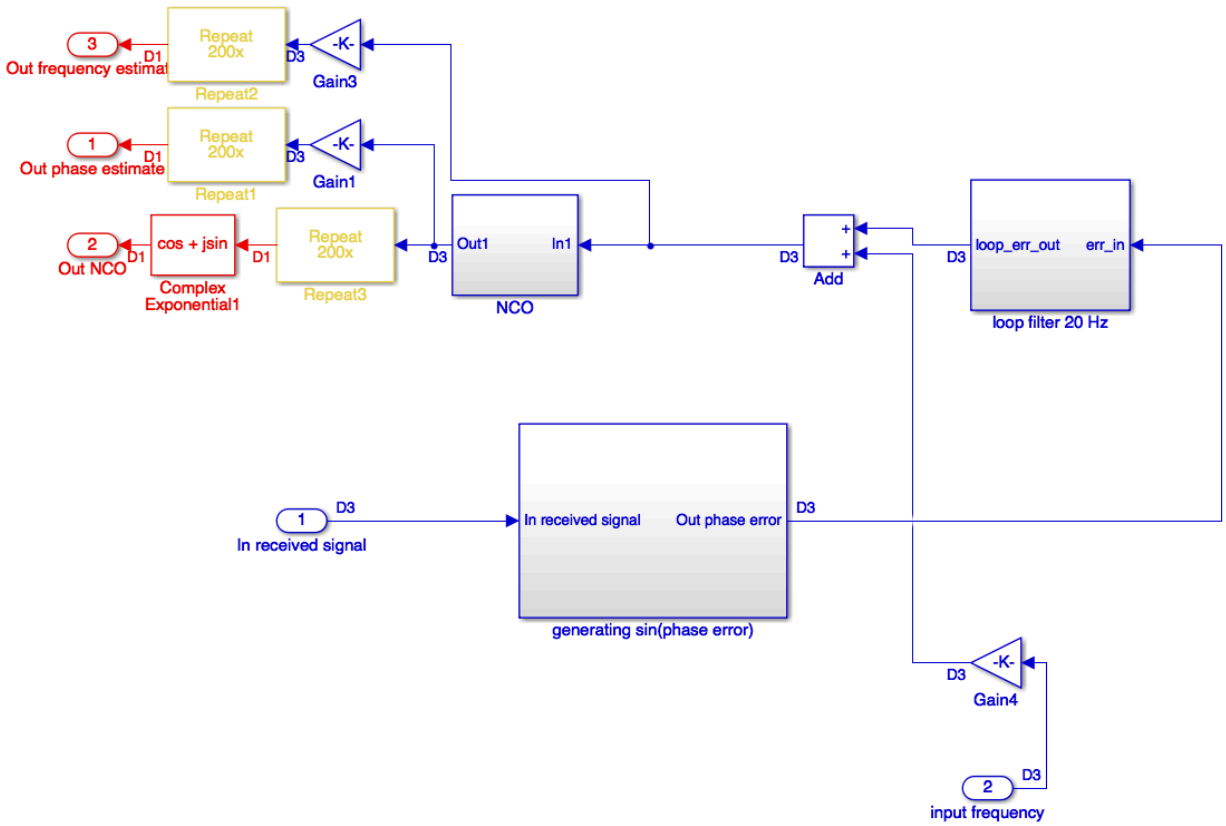

Fig. 13 PLL Circuit

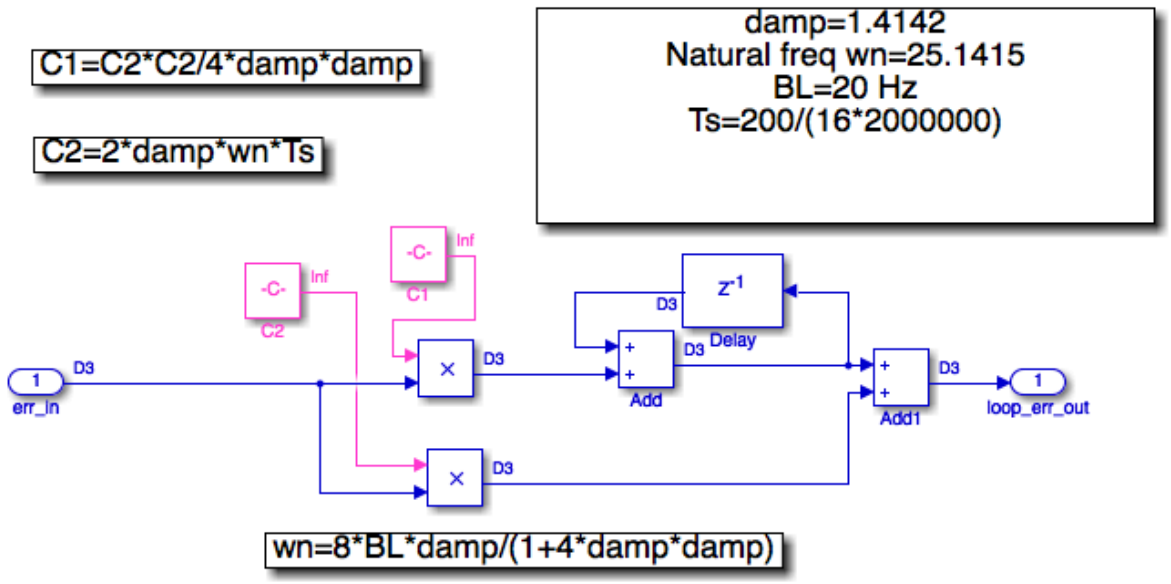

Fig. 14 Loop filter circuit

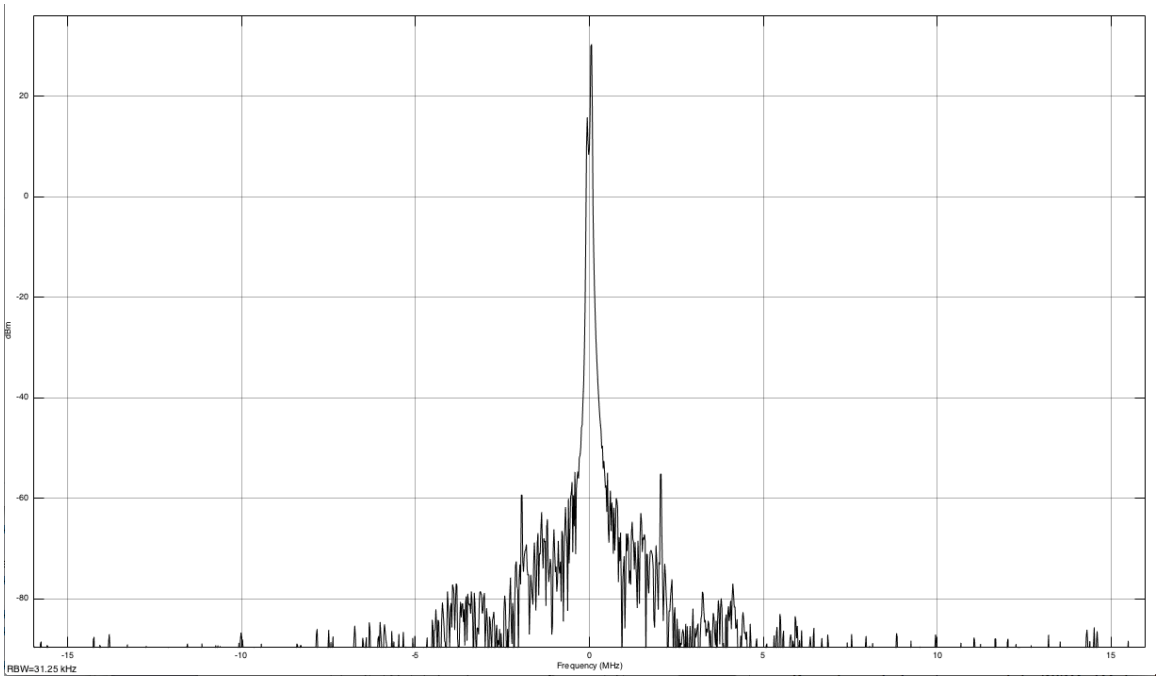

Fig. 15 Spectrum at the output of low pass filter

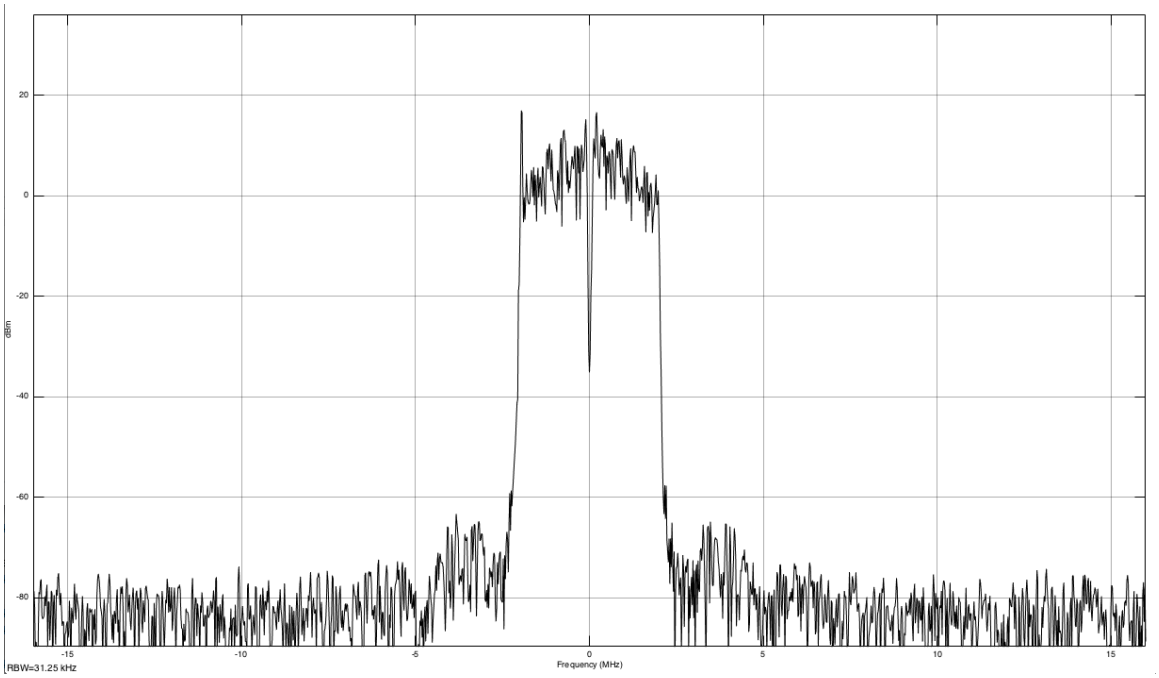

Fig. 16 Spectrum at the output of bandpass filter for PN filtering and downlink modulation

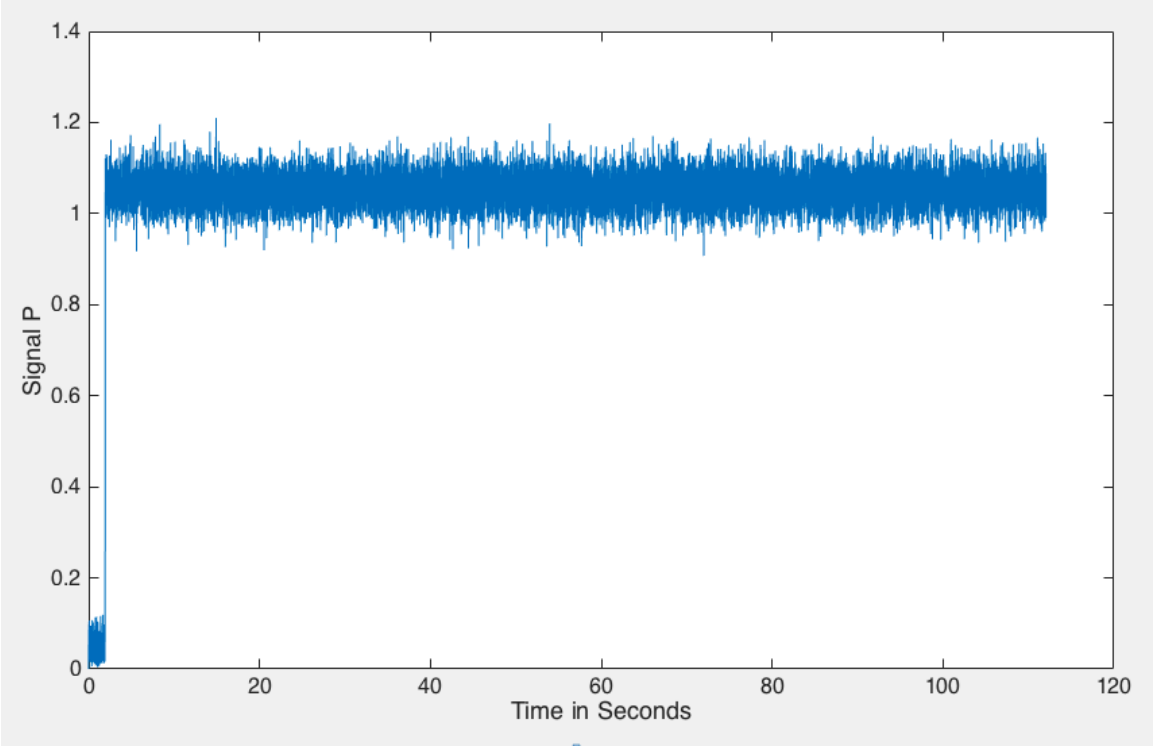

Fig. 17 Lock detection signal P during frequency acquisition and tracking

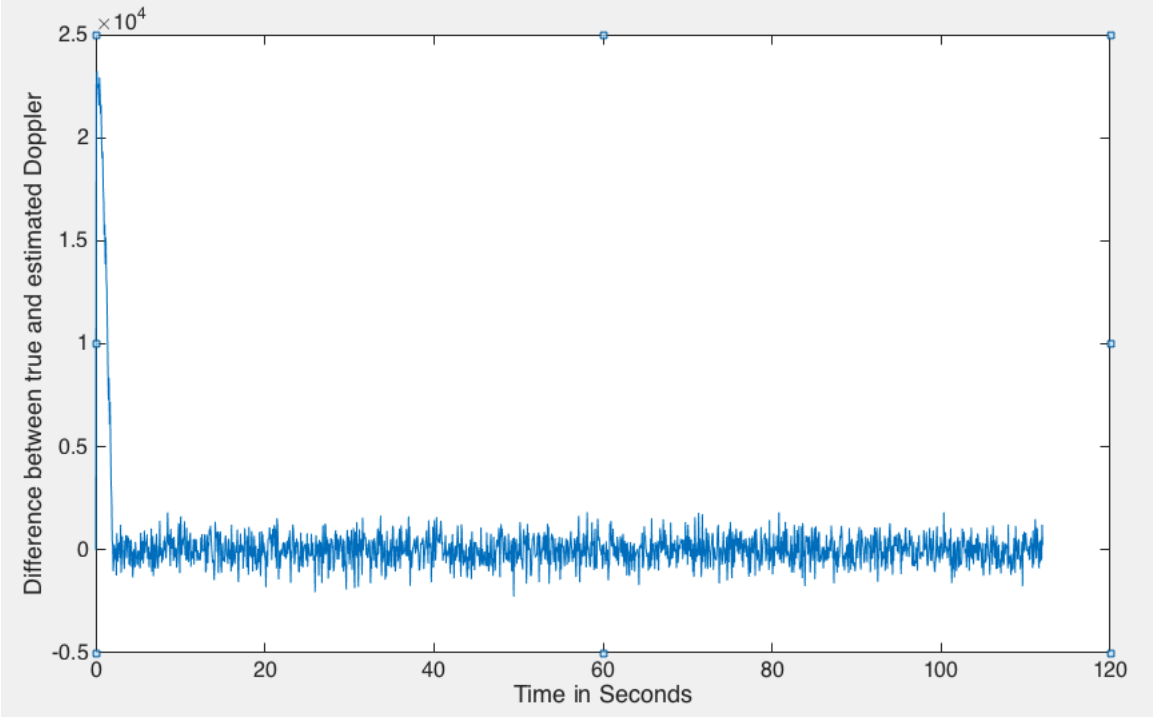

Fig. 18 Difference between Doppler and estimated Doppler during frequency acquisition and tracking. The sign of this difference represents the signal q

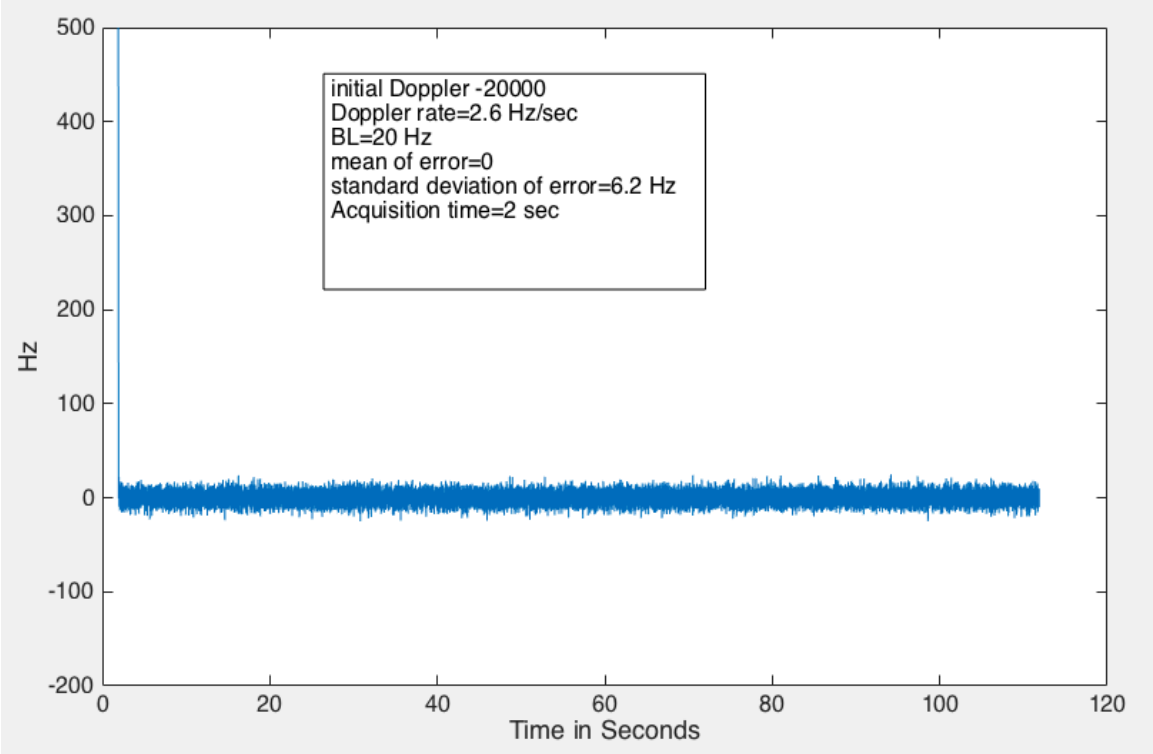

Fig. 19 Frequency tracking error after acquisition

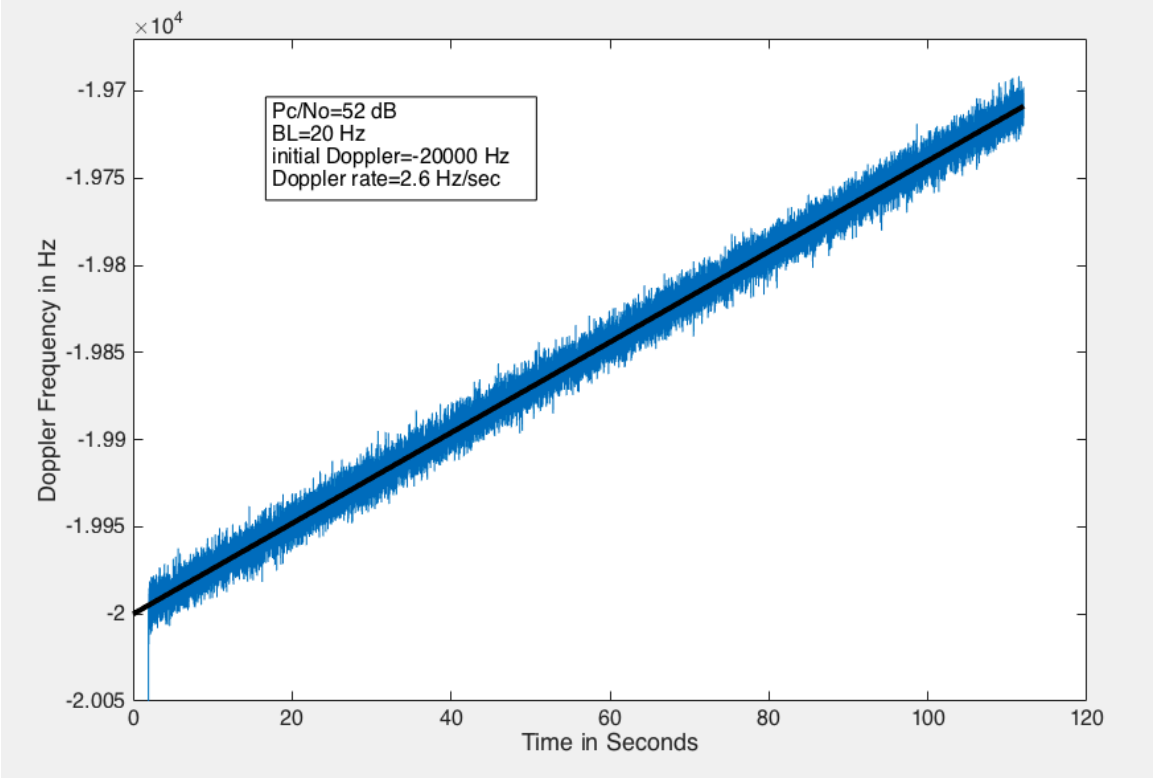

Fig. 20 Doppler and estimated Doppler

VII. Concluding Remarks

In this paper, a two-way Doppler and ranging scheme for navigation tracking for multiple orbiting spacecraft at Mars is described. This scheme does not require any changes to the current DSN ground signal processing, and only needs multiple copies of the Receiver Ranging Processors (RRPs) at the ground station to measure the Doppler frequency and to estimate the range for each of the downlink streams. On the spacecraft side, due to the partial Doppler compensation of the uplink, the flight radio would experience higher Doppler and Doppler rate residuals. We introduce a smart frequency sweeping algorithm that acquires and tracks the more dynamic uplink signals experienced by each spacecraft.

We illustrate the application of this scheme to support simultaneous OD for the Mars orbiters of a notional Mars Regional Navigation Satellite System (MRNSS). We generate the residual Doppler and Doppler rate profiles of the Mars orbiters using different Doppler compensation strategies. We simulate the Doppler acquisition and tracking performances and demonstrate the feasibility of this collaborative flight-ground navigation tracking architecture.

VIII. Acknowledgement

The research described in this paper was carried out at the Jet Propulsion Laboratory, California Institute of Technology, under a contract with the National Aeronautics and Space Administration (NASA). The research was supported by the NASA Space Communications and Navigation (SCaN) Program.

IX. References

[1] Cheung, K., Lee, C., "In-Situ Navigation and Timing Services for a Human Mars Landing Site Part 1: System Concept," September 2017, *68th International Astronautical Congress*, Adelaide, Australia.

[2] Cheung, K., Divsalar, D., and Bryant, S., "Two-Way Ranging and Doppler for Multiple Orbiting Spacecraft at Mars," *IEEE Aerospace Conference 2018,* Big Sky, Montana, March, 2018.

[3] Abraham, D., et. al., "Enabling Affordable Communications for the Burgeoning Deep Space CubeSat Fleet," *SpaceOps 2016, Daejeon*, S. Korea, May 2016.

[4] Abraham, D., et. al., "Deep Space Capacity Study – Pass 2," JPL internal report.

[5] Divsalar, D., Cheung, K., et. al., "CDMA Communication System Performance for a Constellation of CubeSats around the Moon," *IEEE Aerospace Conference 2016,* Big Sky, March 2016.

[6] Berner, J., Bryant, S., and Kinman, P., "Range Measurement as Practiced in the Deep Space Network," *Proceedings of the IEEE*, Vol. 95, No. 11, November 2007.

[7] Edwards, C., Jedrey, T., et al., "The Electra proximity link payload for Mars relay telecommunications and navigation, IAC-03-Q.3.A06," *International Astronautical Congress 2003*, Sep.–Oct. 2003.

[8] "Autonomous Software-Defined Radio Receivers for Deep Space Applications," Jon Hamkins (Editor), Marvin K. Simon (Editor), Joseph H. Yuen (Series Editor), ISBN: 978-0-470-08212-6, Oct 2006, John Wiley & Sons.